

Coherent State Monitoring in Quantum Dots

Ameenah N. Al-Ahmadi and Sergio E. Ulloa

Department of Physics and Astronomy, and Nanoscale and Quantum Phenomena Institute, Ohio University, Athens, OH 45701-2979

(Dated: November 20, 2018)

We study the dynamics of excitonic states in dimer and trimer arrangements of colloidal quantum dots using a density matrix approach. The dots are coupled via a dipole-dipole interaction akin to the Förster mechanism. Coherent oscillations of tuned donor dots are shown to appear as plateaus in the acceptor dot, and therefore in its optical response. This behavior provides one with an interesting and unique handle to monitor the quantum state of the dimer, an “eavesdropping arrangement.” A trimer cluster in a symmetrical loop shows steady states in a shorter characteristic time than the typical radiative lifetime of the dots. Breaking the symmetry of the loop results again in damping oscillatory states in the donor dots and plateaus in the eavesdropping/acceptor dot. The use of realistic parameters allows direct comparison with recent experiments and indicates that coherent state monitoring is possible in real experiments.

PACS numbers: 71.35.-y, 78.47.+p, 78.67.-n, 78.67.Bf

Keywords: energy transfer, colloidal quantum dots, Rabi oscillations

The individual optical and electronic properties of quantum dots (QDs) can be controlled by their size, shape, and composition.^{1,2} Optical studies on different QD systems, such as CdSe,^{3,4} CdS,⁵ and InP,⁶ have revealed information about the coupling between collections of dots. This coupling may take place via direct charge transfer (tunneling), and/or via long-range energy transfer or Förster interaction, in which excited donor (D) dots transfer their energy to unexcited acceptor (A) dots. Förster developed the theoretical treatment of energy transfer in organic molecules,⁷ and is now routinely observed even in molecular self-assembled layers.⁸ This theory assumes that the energy transfer arises from dipole-dipole interaction. Although higher multipolar interactions are possible in principle, they are negligible in typical systems,⁹ but important in others, such as closely packed metal nanoparticles.¹⁰ Förster derived an expression for the resonant energy transfer rate between donors and acceptors, $K_{DA} = (2\pi/\hbar)V_F^2\Theta$, where

$$V_F = \frac{\mu_D\mu_A}{\epsilon R^3}\kappa. \quad (1)$$

Here, μ_D (μ_A) is the dipole moment of the donor (acceptor), R is the separation between D and A centers, ϵ is the dielectric constant of the medium. κ is an angular dipole orientation factor; assuming the dipole orientations for D and A to be (anti- or) parallel, we set $\kappa \simeq 1$. Θ is the spectral overlap integral between normalized donor emission and acceptor absorption lineshapes. Energy transfer between QDs has been verified in beautiful experiments by different groups,^{3,4,11,12} opening a number of interesting possibilities. For example, one can consider the low-temperature non-dissipative coupling between dots and the corresponding coherent oscillations describing excitation transfer. This provides one with a new tool to control the coherent state of an optical excitation in the QDs, controllably monitor coherent spin transfer between dots,^{12,13} and possibly new physical implementations of quantum computation concepts.

In this paper we use a density matrix approach to study the dynamics of exciton states in dimer and trimer arrangements of colloidal quantum dots. We consider that each quantum dot has two main exciton states, one optically passive (dark) and another active (bright), to account for the well-known symmetries in II-VI nanocrystals.¹ The dots are assumed to be in close proximity, thanks to molecular linkers or spacers that allow dipolar coupling but yet prevent direct carrier hopping. We analyze the time evolution of each exciton state after different pumping pulses, and for different structural parameters. We find, for example, that at low temperatures and for realistically attainable systems, one could monitor the coherent oscillations between neighboring (and nearly identical) dots using an “eavesdropping” acceptor dot nearby. The monitoring acceptor dot is shown to exhibit periodic photoluminescence (or absorption) plateaus in the sub-nanosecond regime, and only weakly (although irretrievably) affecting the coherent oscillations in the sympathetic dimer. We also explore other geometries and regimes and show how one can exploit the flexibility in dot cluster features to probe the quantum mechanical states of these systems.

Theory and Model. We use a Markovian equation to describe the dynamics of the exciton states in the QD system

$$\frac{\partial \hat{\rho}_{ij}}{\partial t} = -\frac{i}{\hbar}\langle i | [\hat{H}, \hat{\rho}] | j \rangle - \sum_{lk} \Gamma_{lk,ij} \hat{\rho}_{lk}, \quad (2)$$

where \hat{H} and $\hat{\rho}$ are the Hamiltonian and density operators, respectively, and $\Gamma_{lk,ij}$ is the relaxation matrix.¹⁵ The Hamiltonian that describes the system is the excitonic Hubbard model given by¹⁴

$$H = \sum_i^N U_i c_i^\dagger c_i d_i^\dagger d_i + \sum_{i \neq j}^N V_{F^{i_n j_m}} c_{i_n}^\dagger d_{i_n}^\dagger d_{j_m} c_{j_m}, \quad (3)$$

where U_i is the binding energy of the exciton in the dot,

c^\dagger and d^\dagger are electron and hole operators, and $V_{Fi_nj_m}$ is the coupling constant that governs the exciton energy transfer between level n of dot i and level m of dot j . The coupling constant in principle includes all possible mechanisms that allow the energy transfer to take place. This Hamiltonian can describe, for instance (with the possible addition of phonon degrees of freedom), how the energy moves among donors before emission occurs (exciton migration),¹⁶ or how the excitation transfers irreversibly from donor to acceptor and is then emitted out of the system as a real photon (Förster transfer).⁷ We will focus here on the coherent coupling between dots (a low temperature regime). The dipole moments entering $V_{Fi_nj_m}$ are modeled by a hard wall confinement potential, proven successful in the description of colloidal quantum dots.¹ We correct the overestimation of the exciton energy ground state for small sizes by rescaling the gap to match the experimental results.¹⁷ For simplicity, the dot is assumed to have two exciton levels. The high-energy bright level (absorbing line) has a rapid relaxation rate ($\lesssim 1$ ps at ~ 10 K) to the dark (low-energy) level (emitting line) as known from experiments [see inset (b) of Fig. 1]. The lifetime of the dark level is much longer (~ 20 ns) than the time scale of our calculations (~ 1 ns). The linewidth of the dark states becomes then negligible in the time window of interest. We should mention that inclusion of a more detailed level description of the dots is straightforward, although not essential for our conclusions, as we will see. The experimental values obtained from the luminescence data of the exciton in CdSe nanocrystals are used to estimate the coupling constants.¹⁸

Dimer. Consider first the dynamics of a *dimer* consisting of a donor and acceptor dot pair (such as the D_2 - A pair in the insets in Fig. 1). The system may be reduced to three main levels, neglecting the bright exciton level of the donor dot because of its characteristic fast relaxation time. The exact analytical solution of such a three-level system shows that there is an effective decay of the donor lower level which depends on the coupling V_F (itself a function of dot separation and sizes), the width of the bright exciton state in the acceptor dot Γ_A , and on the detuning ω between the donor dark state and the acceptor bright state. The effective relaxation for weak coupling $V_F \ll \Gamma_A$, is given by the rate

$$\Gamma_{eff} = \frac{V_F^2 \Gamma_A}{(\Gamma_A/2)^2 + \omega^2}, \quad (4)$$

while for $V_F \gg \Gamma_A$, $\Gamma_{eff} \simeq \Gamma_A/2$. The linewidth Γ_A of the exciton levels in a single QD is of course a function of temperature,¹⁹ and QD radius.¹⁸ These equations reveal that a dimer can be thought of and used as a *tunable linewidth* “level” by controlling the coupling V_F , either by changing the distance between donor and acceptor dots or by changing their sizes (which changes ω and weakly Γ_A). Notice that the dark level in the donor dot transfers energy to the acceptor bright state as a *virtual* (non-radiative) process.²⁰

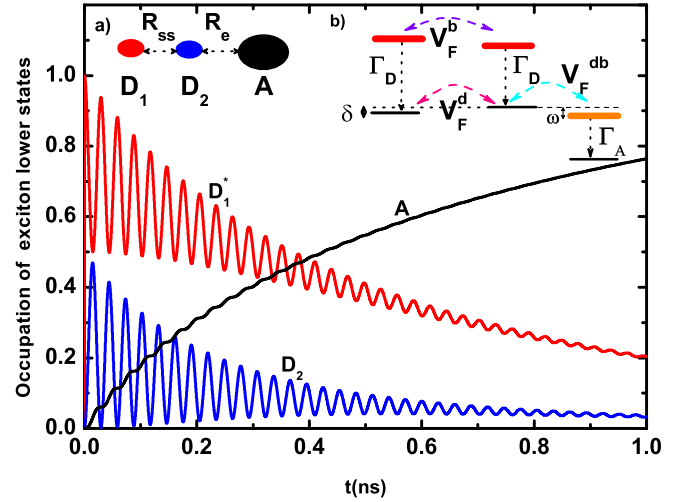


FIG. 1: Time evolution of occupation probability of lower exciton state in each dot. Parameters used are $V_F^d = -0.05$ meV, $V_F^b = -1$ meV, $V_F^{db} = -0.21$ meV, $\Gamma_D = 32$ meV, $\Gamma_A = 30.5$ meV, $\delta = \omega = 0.1$ meV, and $R_{ss} = R_e = 11\text{\AA}$. Inset (a) shows diagram of trimer chain and (b) corresponding energy diagram. Donor dot D_1 has been excited at $t = 0$. Notice plateaus in occupation of dot A.

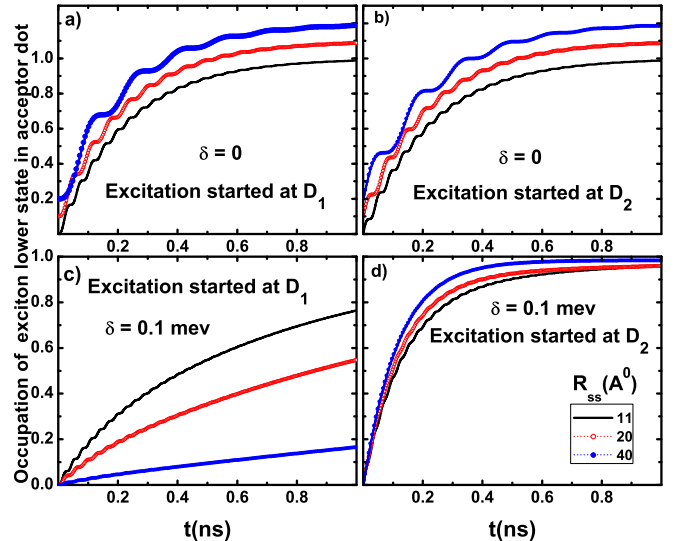


FIG. 2: Dynamics of exciton lower state occupation of acceptor dot for different R_{ss} values ($R_e = 11\text{\AA}$ fixed as in Fig. 1). (a) Initial excitation (pumping) of D_1 for $\delta = \omega = 0$. (b) Pumping D_2 , $\delta = 0$. (c) Pumping D_1 , $\delta = 0.1$ meV. (d) Pumping D_2 , $\delta = 0.1$ meV. Curves in (a) and (b) are offset vertically for clarity. Notice large variation in characteristic growth times, as well as plateaus for nearly all conditions.

Linear Trimer. Let us consider two donor dots coupled to a third acceptor dot, forming a trimer. Figure 1 shows the oscillations in occupation of the different exciton *lower* states in each dot after the first donor dot (D_1) is resonantly excited. All six levels in the system have been used in the numerical solution of the density

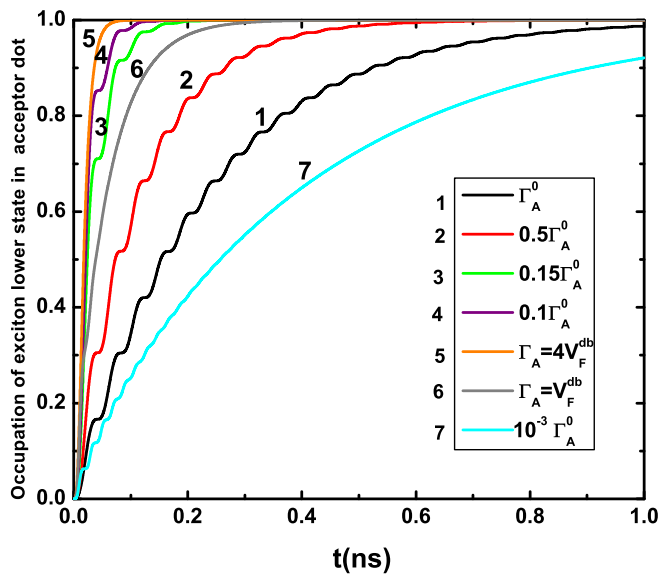


FIG. 3: Dynamics of exciton lower state population at the acceptor dot with varying Γ_A . $\Gamma_A^0 = 30.5$ meV as in Figs. 1 and 2. Notice absence of oscillation plateaus and fastest rise time for $\Gamma_A = 4V_F^{db}$.

matrix evolution. The red and blue curves represent the low energy exciton level for the first and second donor dot, respectively. The black curve is for the acceptor lower state. It is clear that the coupling between the donor lower states V_F^d , induces coherent oscillations of the exciton population in the donor pair, despite the small detuning δ between the low energy donor states. These oscillations show a period $\tau_F^d \simeq h/\sqrt{\delta^2 + 4V_F^{d^2}} = 29$ ps, with an overall slow decay, also seen as growth in the acceptor dark state, with a rise time $\simeq 0.7$ ns. Most importantly, the acceptor is shown to act as a nearly ideal “eavesdropping” point that can effectively monitor coherent oscillations between the two donor dots without totally collapsing them: The coherent oscillations between the nearly tuned donors appear as plateaus in the acceptor dark level population with the same time period of 29 ps. These plateaus persist over the first 0.3 ns, and could possibly be monitored by time-resolved differential absorption measurements of the acceptor state.

The effects of interdot separation on the dynamics of the lower acceptor dot state are shown in Fig. 2 for different pumping conditions. Increasing the separation R_{ss} between the surfaces of the two donors, D_1 and D_2 in Fig. 1, reduces the coupling constant as $(a_1 + a_2 + R_{ss})^{-3}$, where a_1 (a_2) is the radius of D_1 (D_2). The oscillation period is longer for larger R_{ss} since V_F^d becomes smaller, and fewer plateaus appear in the low energy state of A over the same time interval. Notice that the D_2 - A distance in the trimer remains constant throughout Fig. 2; larger R_e separations would result in less defined plateaus in the growth curves in Fig. 2. The behavior is slightly different when we start the excitation in either the first

or second donor, D_1 or D_2 , as shown in Fig. 2a and 2b. In these cases the growth rate remains nearly constant ($\simeq \Gamma/2$ or 0.24 ns, with Γ as in Eq. 4), as it is related to the coupling between D_2 and A kept fixed, while the oscillation period changes with R_{ss} . Notice also that there is a delay time for the appearance of the first plateau in 2a which is different in each case. This delay time, ~ 13 ps, corresponds to the accumulation time of the amplitude occupying the lower exciton level in D_1 . Panels (c) and (d) of the figure represent two donors with a slightly different size and corresponding detuning $\delta = \omega = 0.1$ meV. Notice that a small detuning allows one to spectrally select which of the two donor dots is actually pumped in experiments, so that different initial conditions can be tested. The occupation of the lower exciton state in the acceptor dot exhibits here *different* overall slopes that rapidly increase with decreasing R_{ss} , as shown in Fig. 2c in the case of D_1 pumping. It is clear that weaker coupling (larger R_{ss}) between D_1 - D_2 results in slower building up of the amplitude in A , as one would expect. Moreover, the number and amplitude of the plateaus decrease for larger R_{ss} . In contrast, the dynamics in 2d, after exciting D_2 , shows minor changes in slope (given by Eq. 4, $\simeq 0.12$ ns), and also clear disappearance of the plateaus as the distance R_{ss} increases. This behavior can be understood by analogy to Rabi oscillations, where the Rabi period must be shorter than the effective decay given by the homogeneous linewidth Γ_{eff} . The detuning increases the Rabi frequency, but slows the growth rate of occupation of the acceptor lower state. The strong R_{ss} dependence shown here emphasizes the need for close and well-controlled proximity of the D_1 - D_2 separation. As experiments in this field show outstanding control, one would expect that this requirement is easily fulfilled.

In Fig. 3 we plot the probability of finding the exciton in the acceptor dot in the trimer for different values of the linewidth of the acceptor bright state. The occupation of the acceptor low-energy state grows exponentially with time, and the effective growth rate increases with decreasing linewidth Γ_A . It is interesting that decreasing Γ_A results in a *total suppression* of the coherent plateaus at a special value $\Gamma \simeq 4V_F^{db} \simeq 1$ meV (more on these and related values below). Further decreasing Γ_A results in a smaller growth constant and the plateaus becoming visible again. For a description of this behavior we divide the relative values of Γ_A and V_F^{db} into three regions: $\Gamma_A \gg V_F^{db}$, $\Gamma_A \sim 4V_F^{db}$, and $\Gamma_A \ll V_F^{db}$. In the first region, where $V_F^d, V_F^{db} \ll \Gamma_A$, the analytical solution of the dimer may be employed to reduce the second donor and acceptor to a two-level system having an effective damping given by Eq. (4). Therefore the D_1 - D_2 coherent oscillation frequency V_F^d faces this effective damping, as in the case depicted in Figs. 1 and 2. In the second region, where $\Gamma_A \sim 4V_F^{db}$, the oscillation and plateaus are suppressed, as the effective oscillation frequency is vanishingly small, and only a smooth damping persists. In the last region, where $\Gamma_A \ll V_F^{db}$, the coherent oscillations reoccur and the oscillation survives a damping rate

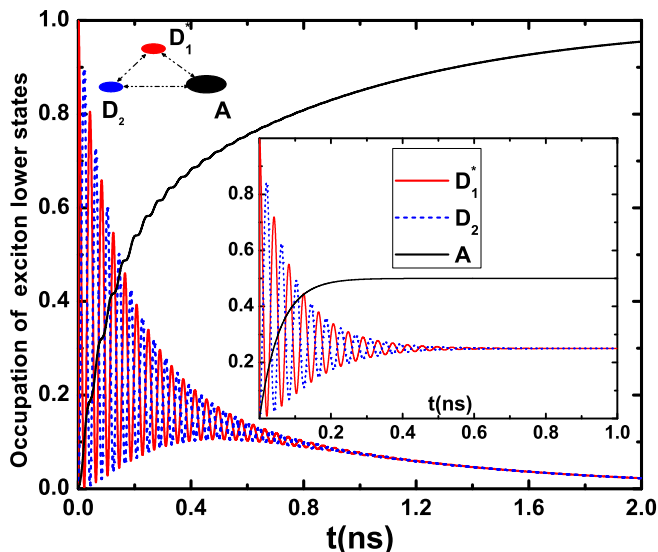


FIG. 4: Evolution of lower exciton state at each dot arranged in an asymmetrical cluster loop as shown in top left inset. Oscillation plateaus are visible in eavesdropping A dot. Central inset shows results for a *symmetrical* loop; notice absence of plateaus in the A -response and saturation at $\frac{1}{4}$ -filling in this time window.

equal to $\Gamma_A/2$. From this result and those above, it is clear that changing the system parameters changes the effective damping of the excitation in the donor. Doing this, one can control the relative coupling between donors and the effective damping of the nearby dimer. For example, the coupling constant of the two lower states in the donor is $V_F^d = -0.05$ meV and the effective damping for our dimer is $5.8 \mu\text{eV}$, resulting from a Förster coupling of 0.21 meV for $R_e = 11 \text{ \AA}$ between donor and acceptor dots. Making the D_2 - A dot surfaces touch we can increase the coupling to ~ 0.7 meV, which gives an effective damping of ~ 0.06 meV and hence we can reduce the interaction V_F^d to a value less than the effective damping. In this example, the interval above and below the resonant condition $\Gamma_A \sim 4V_F^{db}$ can be covered in experiments.

Trimer Cluster. In Fig. 4 we explore the arrangement of a trimer arranged as a cluster “loop,” with two identical donor dots and an acceptor that has a bright ex-

citon level in resonance with the lower exciton level in the donors and is coupled to both dots. The central inset shows results for the symmetric case in which the distances between dots are identical. This symmetrical loop shows essentially *steady* states of the donor and acceptor dots in a characteristic time that is less than the typical radiative time of the dots. This surprising lack of oscillation plateaus in A , as well as the long-lasting plateau at quarter-filling in D_1 and D_2 could be a way to test for the symmetry of a cluster sample in experiments. The cancellation of the oscillation plateaus is a natural result of the in-phase (simultaneous) excitation of the D dots and a direct proof of coherent behavior. On the other hand, breaking the symmetry of the loop, as shown in the main curves in Fig. 4, restores damping to the oscillatory behavior in the donor dots and plateaus to the eavesdropping/acceptor dot. The characteristic oscillation period and plateau rising times are similar to the linear arrangements.

Conclusions. We have used the density matrix approach to investigate the dynamics of the exciton lower states in quantum dot clusters arranged linearly and in triangular loops. The dots are coupled via dipole-dipole excitonic interactions, and the energy transfer processes can take place among donor dots, so that the excitation energy may reach an acceptor dot after “hopping” (near) resonantly among donors. Coherent oscillations are induced in donors and they appear as plateaus in the acceptor dot. The acceptor then behaves as a nearly ideal “eavesdropping” observer point that can effectively monitor the oscillations without strongly affecting them. Although our results here are based on a simplified model of the dot, it is clear that the complexity of multilevel dynamics would contribute to increase Γ_A rates slightly but would not affect our main results. We believe this phenomenon allows the possibility of monitoring states where perhaps the spin of the carriers could be effectively initialized via circularly polarized pumping. A description of this and related regimes will be presented elsewhere.

This work was supported by the Indiana 21st Century Fund and the Condensed Matter and Surface Sciences Program at OU. We thank helpful discussions with G. Bryant, J.M. Villas-Bôas, G.P. Van Patten and the Ball State University QD team.

¹ Al. L. Efros, M. Rosen, M. Kuno, M. Nirmal, D. J. Norris, and M. Bawendi, Phys. Rev. B **54**, 4843, (1996); Al. L. Efros and M. Rosen, Ann. Rev. Mater. Sci. **30**, 475 (2000).
² C.B. Murray, C.R. Kagan, and M.G. Bawendi, Ann. Rev. Mater. Sci. **30**, 545 (2000)
³ C. R. Kagan, C. B. Murray, M. Nirmal, and M. G. Bawendi, Phys. Rev. Lett. **76**, 1517 (1996).
⁴ S. A. Crooker, J. A. Hollingsworth, S. Tretiak, and V. I. Klimov, Phys. Rev. Lett. **89**, 186802 (2002).
⁵ T. Vossmeier, L. Katsikas, I. G. Popvic, K. Diesner, A.

Chemseddine, A. Eychmüller, and H. Weller, J. Phys. Chem. **98**, 7665 (1994).

⁶ O. I. Micic, Kim M. Jones, A. Cahill, and A. J. Nozik, J. Phys. Chem. B **102**, 9791 (1998).

⁷ T. Förster in *Modern Quantum Chemistry III*; ed. O. Sinanoglu (Academic, New York, 1965) pp. 93-137.

⁸ A. Painelli, J. Am. Chem. Soc. **125**, 5624 (2003).

⁹ Y. Okuno and S. Mashiko, Int. J. Quan. Chem. **90**, 772 (2002).

¹⁰ R. Rojas and F. Claro, Phys. Rev. B **34**, 3730 (1986).

- ¹¹ M. Achermann, M. A. Petruska, S. A. Crooker, and V. I. Klimov, *J. Phys. Chem. B* **107**, 13782 (2003).
- ¹² M. Ouyang, and D. D. Awschalom, *Science* **301**, 1074 (2003).
- ¹³ A. O. Govorov, *Phys. Rev. B* **68**, 075315 (2003).
- ¹⁴ G. W. Bryant, *Physica B* **314**, 15 (2002).
- ¹⁵ G. Mahler, and V. A. Weberruß, *Quantum Networks: Dynamics of Open Nanostructures* (Springer, Berlin, 1998).
- ¹⁶ B. D. Bartolo, *Energy Transfer Processes in Condensed Matter* (Plenum Press, New York, 1984).
- ¹⁷ C. B. Murray, D. J. Norris, and M. G. Bawendi, *J. Am. Chem. Soc.* **115**, 8706 (1993).
- ¹⁸ D. J. Norris, Al. L. Efros, M. Rosen, and M. G. Bawendi, *Phys. Rev. B* **53**, 16347 (1996).
- ¹⁹ S. A. Crooker, T. Barrick, J. A. Hollingsworth, and V. I. Klimov, **82**, 2793 (2003).
- ²⁰ We should remark that it is well known that the dark lower energy exciton state is not optically active due to its angular momentum $F = \pm 2$.¹ However, this state does have non-zero dipole moment which can then produce a Förster coupling and its energy be (near) resonantly transferred to neighboring dots via virtual non-radiative intermediate states.